31st Congress of the International Council of the Aeronautical Sciences

Belo Horizonte, Brazil; September 09-14, 2018

DIRECT NUMERICAL SIMULATION OF MACH WAVE INFLUENCE ON LAMINAR-TURBULENT TRANSITION IN SUPERSONIC FLOW OVER A FLAT PLATE

I.V. Egorov*,, A.V. Fedorov*, K.H. Ding***

***Moscow Institute of Physics and Technology, ****Central Aerohydrodynamic Institute**

Keywords: *numerical simulation, Mach wave, Tollmien-Schlichting wave*

Abstract

On the base *of three-dimensional Navier-Stokes equations, the influence of Mach waves (N-wave) on laminar-turbulent transition caused by the first mode in the boundary layer on a flat plate is studied numerically at the free-stream Mach number 2.5. In accord with the wind-tunnel experiment N-wave is induced by two-dimensional roughness on the computational domain boundary corresponding to the test section side wall. It is shown that the disturbance induced in the boundary layer by the N-wave rear front, does not affect the transition onset but it shifts the nonlinear stage of the first mode evolution downstream. The disturbance induced by the N-wave fore front, shifts the transition onset upstream.*

1 Introduction

Laminar-turbulent transition (LTT) is substantially depends on free stream disturbances, which have different nature and spectral distribution in wind tunnels (WT) and in real flight conditions. For correct interpretation of wind tunnel results and LTT data transfer to real flight conditions studies of typical disturbances in test section of WT and mechanisms of their interaction with boundary layer on the model surface are necessary. Main sources of disturbances in supersonic WT are turbulent boundary layer and roughnesses on the nozzle walls and test section [1]. Roughnesses lead to generation of weak shock waves (Mach waves), which penetrate into flow core. These waves, interacting with model leading edges, excite disturbances in boundary layer, which may significantly influence on local heat fluxes, viscous friction coefficient and LTT position. Vaganov et al. ([2], [3]) investigated this type of disturbances in wind tunnel T-325 at Mach number 2.5. Source of disturbances was 2D roughness (thin strip), located on the lateral surface of WT test section. As a rule, roughness height was much less than turbulent boundary layer on the WT wall. Nevertheless, Mach waves penetrate into boundary layer and spread to flow core, generating N-wave, intensity of which several times more, than level of natural disturbances. As result of N-wave interaction with leading edge of the thin delta wing ([2], [3]) or plate in laminar boundary layer intensive disturbances of mass flow arise in low-frequency part of the spectrum. Their mean-square level is 2.5 % on the flat plate with sharp leading edge and for the plate with blunted leading edge this level increases to 10%.

Numerical investigations [4] show that profile of longitudinal mass flow in N-wave, obtained from steady solution of Navier-Stokes equations, show good agreement with the experiment.

It can be assumed that distortions of mean (undisturbed) flow, generated by N-wave, may significantly influence on stability, and, as a consequence, on LTT in boundary layer. It is known from (LST) [5] that for non-compressible boundary layer on the flat plate only one unstable mode exists – Tollmien-Schlichting (TS) wave. Its analogue in supersonic boundary layer is referred to as the

first mode according to Mack terminology [5]. In contrast to non-compressible boundary layer, where 2D TS waves have the maximum growth increments, for supersonic boundary layers 3D (oblique) waves are the most unstable. Thus, experiment and theory have to solve the problem of 3D unstable disturbances evolution.

In this work influence of wake, induces by N-wave, on LTT, caused by growth and nonlinear breakdown of the first mode on the sharp plate and is studied numerically. The first mode is artificially excited in boundary layer using periodical suction-blowing through the narrow part of the surface. Main parameters of free stream and the flat plate correspond to the experiment [3].

2 The Problem Statement

Scheme of the problem concerned is shown in Fig.1. Two sources of disturbances are present: the first one generates Mach wave and simulates roughness on the side boundary of computational domain, corresponding to the wall of WT test section; the second one is a generator of unsteady disturbance and located on the plate surface not far from its sharp leading edge.

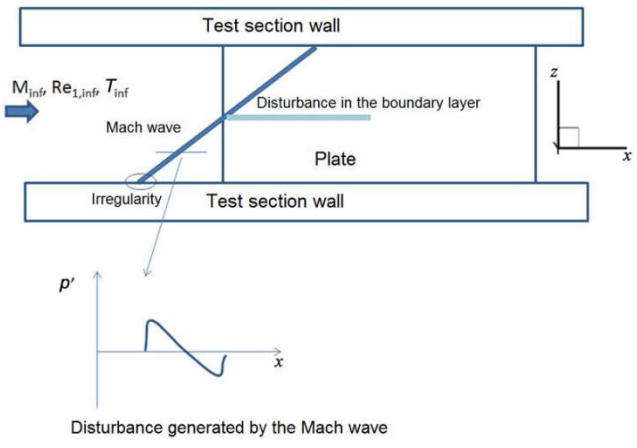

Fig. 1 Scheme of the interaction of the *N*-wave excited by the two-dimensional irregularity on the wind-tunnel side wall with the plate leading edge

All calculation are fulfilled for free stream with Mach number 2.5, unit Reynolds number $Re_1 = 5\times10^6 m^{-1}$ and stagnation temperature 293K. Gas is assumed to be ideal with adiabatic exponent 1.4 and Prandtl number 0.72. Viscosity is calculated using Sutherland formula with constant 110.4 K. The flat plate has temperature of isolated wall. Computational domain and coordinate axes are shown in Fig.2. The size of computational domain in longitudinal direction is L_x=553 mm, in normal to the plate direction - L_y=150 mm and in spanwise direction L_z=200 mm. The plate surface is located in plane (X, Z) at Y=0 and X>0, so that its leading edge has coordinates (X,Y)=(0,0). On the inflow boundary of the computational domain, X = - 260 mm, and on the upper boundary, Y=150 mm, free stream boundary conditions are set. In the region of flow exit buffer zone is located in order to avoid disturbance reflection from the right boundary of the computational domain. On the plate surface (X>0, Y=0) non-slippery boundary conditions and zero heat flux to the wall are set. On the part (X<0, Y=0) and on the side boundaries of computational domain (Z=Zmin=-100 mm and Z=Zmax=100 mm) symmetry boundary condition is set.

N-wave is excited on the side face Z=Zmin at -253 mm <X<-233 mm using boundary conditions, described in chapter 4. These conditions qualitatively simulate disturbance from 2D roughness with width ΔX=20 mm and height ΔZ=0.2 mm.

Unsteady disturbances (mainly the first mode waves) are excited on the plate surface in region 27mm<X<47mm using generator of periodical blowing-suction. Corresponding boundary conditions are given in chapter 5.

Computational grid (see Fig. 2) has approximately 10^8 cells, the number of nodes along coordinates X, Y and Z are N_x=1021, N_y=205 и N_z=481 correspondingly. Near the wall grid is clustered along Y in order to put 100 nodes in boundary layer at section X ≈150 mm. Clustering is also made along longitudinal coordinate X in the vicinity of the plate leading edge X=0 and along transversal coordinate Z, in such a way that wake region contains approximately 120 nodes.

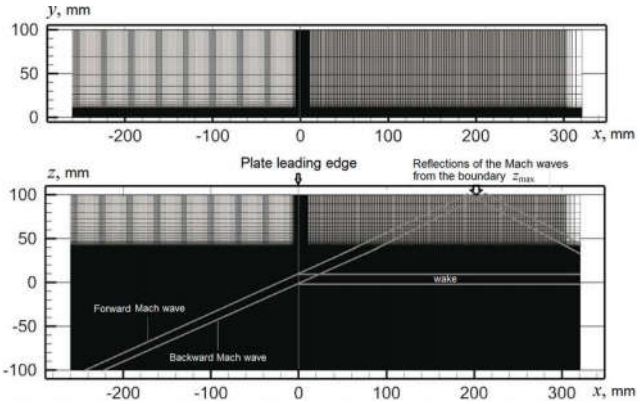

Fig. 2 Numerical grid and boundary conditions.

3 Solution Technique

The papers should be prepared, if possible, using the format like this document Calculation are carried out using HSFlow (High Speed Flow) in-house code [6], where system of 3D unsteady Navier-Stokes equations for perfect gas with constant values of adiabatic exponent and Prandtl number is solved. Fully implicit conservative TVD scheme of second order accuracy in time and space is used for dissipative terms. Convective terms are approximated using third-order WENO scheme [7]. Although this scheme is not high-order accuracy scheme, its numerical dissipation can be decreased by use of rather detailed grid. This allows reliable simulation of such unsteady processes as receptivity and instability of supersonic boundary layers [6], nonlinear development of disturbances in boundary layer on the plate [8] and in zone of laminar separation on the compression corner [9].

Navier-Stokes equations are integrated in non-dimensioned variables: $\bar{x} = X / L$, $\bar{y} = Y / L$, $\bar{z} = Z / L$, $\bar{u} = u / u_\infty$, $\bar{v} = v / u_\infty$, $\bar{w} = w / u_\infty$, $\bar{t} = t\,u_\infty / L$, $\bar{\rho} = \rho / \rho_\infty$, $\bar{p} = p / \rho_\infty u_\infty^2$, $\bar{T} = T / T_\infty$, $\bar{\mu} = \mu / \mu_\infty$.

Reynolds number is $\mathrm{Re} = \rho_\infty u_\infty L / \mu_\infty = 5 \times 10^6$, where L=1 m – characteristic length of the plate.

4 Boundary Conditions for N-Wave Generation

Let on the side boundary $Z = Z_{\min}$ 2D roughness, which is uniform along Y coordinate, is located in region $X_0 < X < X_0 + a$ and has characteristic height $\Delta Z = h$. In local coordinates $z_1 = (\mathrm{Z} - Z_{\min}) / a$, $x_1 = (X - X_0) / a$ roughness is simulated by parabolic arc

$$z_1 = \varepsilon F(x_1), \quad 0 < x_1 < 1,$$
$$\varepsilon = h / a << 1, \quad F(x_1) = O(1)$$

Pressure, velocity and temperature disturbances, induced by roughness in supersonic flow, are calculated according to Ackeret formulas

$$\Delta\bar{p} = \frac{p - p_\infty}{\rho_\infty u_\infty^2} = \varepsilon \frac{F'(x_1)}{\sqrt{M_\infty^2 - 1}} + O(\varepsilon^2)$$
$$\Delta\bar{u} = \frac{u - u_\infty}{u_\infty} = -\varepsilon \frac{F'(x_1)}{\sqrt{M_\infty^2 - 1}} + O(\varepsilon^2)$$
$$\Delta\bar{w} = \frac{w}{u_\infty} = \varepsilon F'(x_1) + O(\varepsilon^2)$$
$$\Delta T = \frac{T - T_\infty}{T_\infty} = \varepsilon \frac{(\gamma - 1) M_\infty^2 F'(x)}{\sqrt{M_\infty^2 - 1}} + O(\varepsilon^2)$$

Relative height of roughness ε = 0.01 is chosen according to the experiment [2]. Disturbances are set as boundary conditions on the side face of computational domain, Z=$Z_{\min}$, at X_0=-233 mm and a = 20 mm. In calculation process steady disturbed flow field is found with high accuracy (residual is less than 10^{-10}). In result weak N-wave is generated, which is schematically shown in Fig. 2. This disturbance develops along Mach lines, reaches the side boundary Z=$Z_{\max}$ and reflects from it.

5 Boundary Conditions for First Mode Excitation

On the narrow region of the plate $x_1 < x < x_2$ boundary condition for normal to the wall mass flow component is set:

$$\left(\rho v\right)'(x_p, y=0, z, t; \beta, \omega, \phi) = A(t) v_p(x_p) \cos(\beta z + \phi) \sin(\omega(t - t_0))$$

$$x_p = \frac{2x - (x_2 + x_1)}{x_2 - x_1},\ x_1 \le x \le x_2 \Rightarrow -1 \le x_p \le 1, t > t_0$$

where x coordinate is measured from the leading edge of the plate, ϕ – is initial phase of the excitation. If $\phi = 0$ excitation is distributed along z in a symmetrical way relative to line $z = 0$. Symmetry line can be shifted in transversal direction increasing ϕ. Excitation shape is given by 5th order polynomial

$$v_p(x_p) = 1.5^4 \left(1 + x_p\right)^3 \left(3\left(1 + x_p\right)^2 - 7\left(1 + x_p\right) + 4\right),$$
$$-1 \le x_p \le 0,$$
$$v_p(x_p) = -1.5^4 \left(1 - x_p\right)^3 \left(3\left(1 - x_p\right)^2 - 7\left(1 - x_p\right) + 4\right),$$
$$0 \le x_p \le 1$$

At initial time moment t_0 excitation amplitude is switched on according to the law

$$A(t) = \lambda\left[1. - \exp(-2\tilde{t}^2)\right],\ \tilde{t} = \omega(t - t_0) / (2\pi)$$

in such a way that signal $A(t)$ reaches the constant level λ after the first two periods of generator oscillations.

Characteristics of the first mode are calculated using LST, and generator parameters are chosen, for which effective instability excitation takes place: ω = 164.66, β = 561.93. Central line coordinate of the generator is located at instability point of this wave: X_0 = 37 mm. Dimensionless coordinates of generator boundaries are chosen in a following way:

$$x_1 = x_0 - \lambda_{TS} / 2,\ x_2 = x_0 + \lambda_{TS} / 2,\ \lambda_{TS} = 2\pi / \alpha_{TS,r}$$

where $\alpha_{TS,r}(\omega, \beta)$ = 305.46 – real part of the first mode eigenvalue, specifying longitudinal component of the wave vector. In dimension form λ_{TS}^* = 20 mm, X_1 = 27 mm and X_2 = 47 mm. Generator amplitude is chosen equal to λ = 0.1% in such a way that nonlinear breakdown occurs inside the computational domain. Calculations are fulfilled in three stages. At first steady flow field without N-wave and unsteady disturbances is calculated. Then at time moment t_1 = 0.75 (after the unsteady flow field becomes stationary with high accuracy) boundary conditions for N-wave excitation are switched on. Calculations are carried out while disturbance, arising because of N-wave interaction with boundary layer on the plate, doesn't come out the computational domain through its right boundary (this takes place to the moment t_2 = 1.8). In result stationary flow field is obtained, containing N-wave and wake, excited by the wave in boundary layer. Then generator of periodical blowing-suction is switched on the plate surface, which effectively excites the first mode. Calculations are carried out until solution approaches stationary unsteady regime, i.e. until initial disturbances, arising at the moment of the generator switching on, leave computational domain through the right boundary. Note that for stationary regime regions of linear and nonlinear disturbance growth do not change their location in space.

6 Results of Calculations

Let us consider disturbance, excited by N-wave in the flow and in boundary layer on the flat plate. In Fig. 3 temperature distribution in plane (X, Z) at Y=0.55 mm is shown. As a result of N-wave interaction with leading edge of the plate wake is formed in the plate boundary layer. Width of the wake in z-direction is nearly constant, and its intensity slowly decreases downstream. In region Z > 0 reaction of boundary layer on N-wave, propagating over the plate, is seen. Red strip indicates region of blowing-suction generator, exciting the first mode.

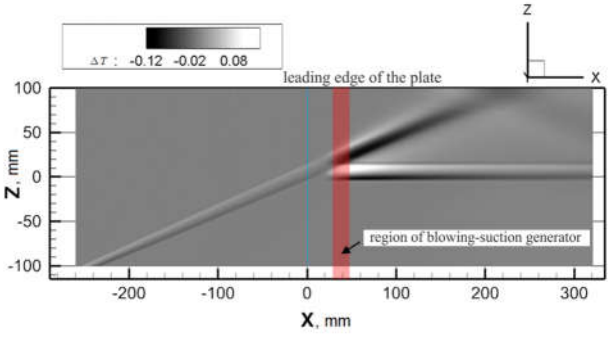

Fig. 3 Distribution of disturbance temperature along the plate surface at Y=0.55 mm.

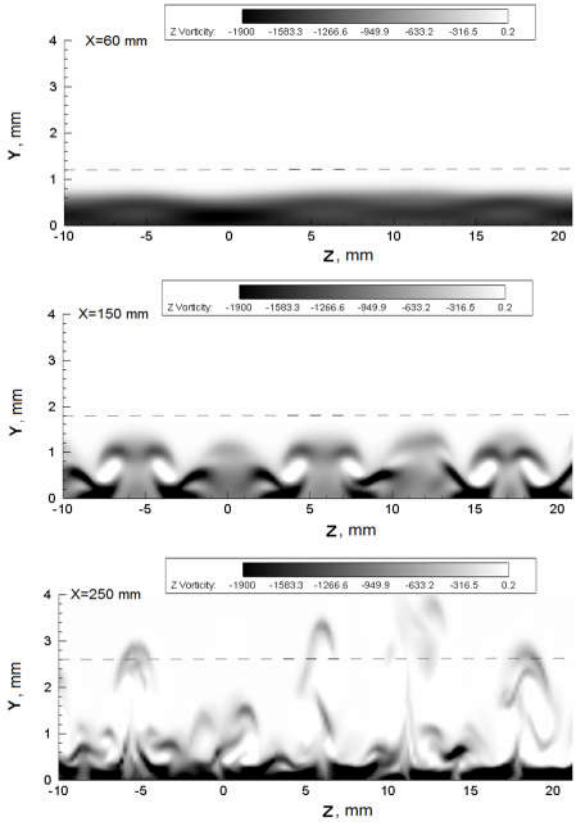

Fig. 4 Transversal vorticity component in sections X = 60 mm, 150 mm and 250 mm.

In Fig. 4 fields of transversal (Z) component of vorticity in sections X=60 mm, 150 mm and 250 mm are shown. In the first section disturbance has small amplitude and is hardly seen in the figure. In the second section downstream (see section X=150 mm) unsteady disturbance, corresponding to the first mode, becomes more intensive and gains arranged mushroom-like structure. Further disturbance enhancement leads to breakdown of orderliness and development of small-scale structures in section X=250 mm. Here disturbances in the region of rear (Z = -0.5 mm) and forward (Z = 11.8 mm) front differs appreciably from each other. Namely, in the region of forward front disturbance enhancement is observed, and in the region of the rear front – disturbance damping. This is well seen in Fig. 5, where fields of transversal vorticity component in sections Z = 11.8 mm and -0.5 mm are given.

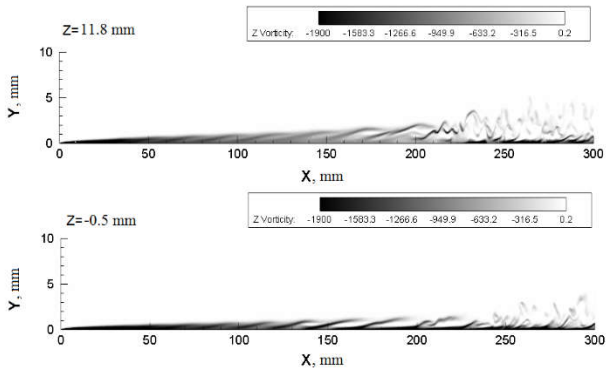

Fig. 5 Transversal vorticity component in sections Z = 11.8mm (forward front) and Z = -0.5 mm (rear front).

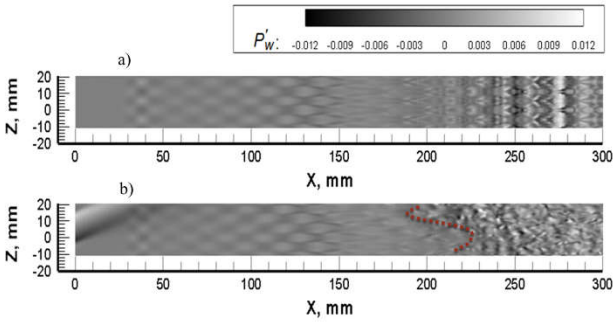

Fig. 6 Pressure disturbance on the flat plate surface: a) – the first mode without N-wave, b) – the first mode with N-wave.

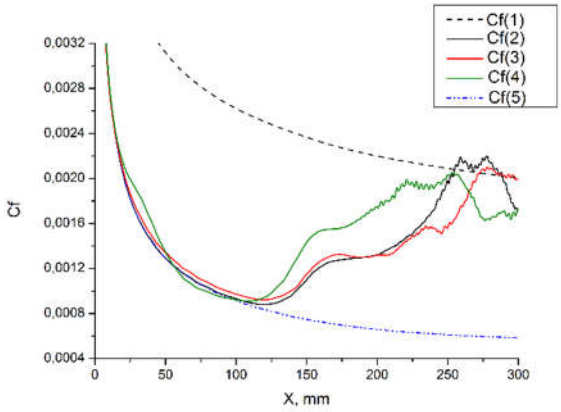

Fig. 7 Distribution of friction coefficient along longitudinal coordinate: *Cf*(1) – turbulent regime; *Cf*(2) – flow with the first mode without N –wave; *Cf*(3) – flow with the first mode and N-wave in the region of rear front; *Cf*(4) – flow with the first mode and N-wave in the region of

forward front; *Cf*(5) – laminar regime.

Distributions of friction coefficient *Cf* along X coordinate for different regions in Z direction are shown in Fig. 7. The curve *Cf*(4) is obtained by averaging on time interval $2.2 < t < 2.3$ and in region -5 mm $< Z < 5$ mm, corresponding to region of disturbances from forward N-wave front. The curve *Cf*(3) is obtained by averaging on interval $2.2 < t < 2.3$ and in region 5 mm $< Z <$ 15 mm, corresponding the region of disturbance from N-wave rear front. Also shown: friction coefficient *Cf*(1) for developed turbulent boundary layer (correlation Van Driest II from [10]); *Cf*(5) for laminar boundary layer; *Cf*(2) (time and Z coordinate averaged) for case without N-wave and only the first mode is excited. It is seen that on earlier stage of the first mode development friction coefficient *Cf*(2) corresponds to laminar boundary layer. Presence of N-wave leads to deviation *Cf*(3) and *Cf*(4) from laminar values. As the development of disturbances downstream progresses LTT zone is formed, where friction coefficient growth takes place. In the region, corresponding to the forward front of N-wave (distribution *Cf*(4)), LTT begins at X = 100 mm. In the region, corresponding to rear front of N-wave (distribution *Cf*(3)) LTT begins at X = 125 mm – approximately at the same location as LTT without N-wave (distribution *Cf*(2)). Coming to turbulent level is viewing at different points: $X \approx 220$ mm for *Cf*(4); $X \approx 270$ mm for *Cf*(3); $X \approx 250$ mm for *Cf*(2).

Thus, disturbance induced in boundary layer by backward N-wave front does not influence on the beginning of boundary layer transition, but moves nonlinear stage development of first mode downstream. Disturbance induced in boundary layer by forward N-wave moves boundary layer transition upstream.

7 Conclusions

Influence of N-wave induced by roughness on the wind tunnel side wall is investigated on the evaluation of the first unstable mode in the boundary layer for flow about flat plate for supersonic Mach number 2.5. Three dimensional first mode waves are excited by means of harmonic in time boundary condition like that suction-injection on the solid wall. It is simulated laminar-turbulent transitional zone including linear and nonlinear stage of disturbances evaluation. In is considered cases with N-wave and without N-wave.

Steady track evaluating on the large downstream distance is generated by interaction of N-wave with the flat plat leading edge. Two extremes are observed in the crossflow sections (x=const). One of them is induced by the by the backward front of the N-wave, another one is induced by forward front of N-wave. It was observed that the LTT from the forward front of N-wave does not influence on the LTT beginning but moving it downstream. LTT from the forward front of N-wave moves LTT zone upstream.

This work was supported by the Russian Scientific Foundation (project 14-19-00821, fulfillment of computational investigations and analysis of results) and RFBR (project 17-08-00969, the algorithm and programs for numerical simulation development). The results of the work were obtained using computational resources of Laboratory for Mathematical Modeling of Nonlinear Processes in Gas Media at MIPT.

References

[1] Pate S.R. *On boundary-layer transition in supersonic-hypersonic wind tunnels. Theory and application*. AEDC-TR-77-107, Arnold Engineering Development Center, Tennessee, March, 1978.

[2] Vaganov A.V., Ermolaev Yu.G., Kolosov G.L., Kosinov A.D., Panina A.V., and Semionov N.V. Action of incident Mach wave on the field of pulsations in boundary layer of a planar delta wing. *Vestnik NGU, Ser. Fizika*, Vol. 9, No. 1, pp. 29–38, 2014.

[3] Vaganov A.V., Ermolaev, Yu.G., and Kosinov, A.D., "Experimental study of flow structure and transition in the boundary layer of a delta wing with blunted leading edges at Mach numbers 2, 2.5, and 4. *Trudy MFTI*, Vol. 5, No. 3, pp. 164–173, 2013.

[4] Dinh Q.H., Egorov I.V., Fedorov A.V. Interaction of Mach waves and boundary layer at a supersonic flow over a plate with a sharp leading edge. *TsAGI Science Journal*, Vol. 48, No. 4, pp. 1–13, 2017.

[5] Mack L. M. *Boundary-layer stability theory*. Internal Document 900-277. Jet Propulsion Laboratory, Pasadena, California, 1969.
[6] Egorov I.V., Novikov A.V. Direct numerical simulation of laminar–turbulent flow over a flat plate at hypersonic flow speeds, *Computational Mathematics and Mathematical Physics*, Vol. 56, No.6, pp. 1048-1064, 2016.
[7] Jiang G.-S., Shu C.-W. Efficient implementation of weighted ENO schemes, *Journal of Computational Physics*, Vol. 126, No. 1, pp. 202-228, 1996.
[8] Novikov A., Egorov. I. Direct Numerical Simulations of Transitional Boundary Layer over a Flat Plate in Hypersonic Free-Stream, *AIAA Paper* 2016-3952, 2016.
[9] Novikov A., Egorov I., Fedorov A. Direct Numerical Simulation of Wave Packets in Hypersonic Compression-Corner Flow, *AIAA Journal,* Vol. 54, No. 7, pp. 2034-2050, 2016.
[10] Schlichting, H., Gersten, K., "*Boundary layer theory*," Springer, 8th Revised and Enlarged Edition.

Copyright Statement